JOURNAL OF COMPUTATIONAL PHYSICS 35, 100–109 (1980)

Computations of the Axisymmetric Flow between Rotating Cylinders*

RITA MEYER-SPASCHE

Max Planck Institut für Plasmaphysik, D8046 Garching, West Germany

AND

HERBERT B. KELLER

Applied Mathematics 101-50, California Institute of Technology, Pasadena, California 91125

Received February 14, 1979

We study Taylor vortex flows by solving the steady axisymmetric Navier–Stokes equations in the primitive variables (u, v, w, p). Fourier expansions in z, the axial direction, and centered finite differences in r, the radial direction, are used. The resulting discretized equations are solved using the pseudoarclength continuation methods of Keller (in "Applications of Bifurcation Theory" (P. Rabinowitz, Ed.), pp. 359–384, Academic Press, New York, 1977.), which are designed to detect bifurcations. In this way we accurately determine the first branch of Taylor vortex solutions bifurcating from Couette flow for both a wide and a narrow gap. Agreement with experiments is extremely good for the wide gap case and solutions are obtained for a larger range of Reynolds numbers than previously reported.

1. INTRODUCTION AND FORMULATION

For sufficiently small Reynolds numbers, Re, the only steady flow of a viscous incompressible fluid between concentric rotating cylinders is the Couette flow:

$$u(r, \theta, z) = w(r, \theta, z) = 0, \qquad v(r, \theta, z) = ar + b/r. \tag{1.1}$$

The constants a, b are determined by the radii and rotation rates of the cylinders. As Re is increased above some critical value, Re_{cr}, the flows of this family become unstable and are replaced by those of another family of solutions containing Taylor vortices (see [1, Fig. 15]). That is, the Taylor vortex solutions bifurcate from Couette flows at $Re = Re_{cr}$. This bifurcation has been studied both numerically and analytically (see [3, 9, 11, 14, 15] and references therein). We present here a new computational study of this bifurcation and of the branch of Taylor vortex solutions that form as Re increases above Re_{cr}. The numerical techniques we use are quite different from those that have been used previously on this problem and they enable us to get

* This research was supported under DOE Contract No. AT-04-3-766.

0021-9991/80/040100–10$02.00/0

accurate bifurcated solutions beyond those previously obtained. We use the primitive variables (u, v, w, p), and the value of Re_{cr} is obtained during our continuation procedure without appeal to the linearized stability theory or to any special bifurcation theory expansions. We formulate the problem below, the numerical methods are described in Section 2, and the results of two series of calculations are presented and discussed in Section 3.

Let the cylinders have radii R_1 and R_2 and gap width $\Delta \equiv R_2 - R_1$. The flow is assumed to be axisymmetric and periodic in the axial or z-direction; say, with period

$$L = 2\pi R_1/k,$$

where k is the axial wave number. Dimensionless variables are introduced using R_1 as the length scale and $\omega_1 R_1$ as the velocity scale (ω_1 is the angular velocity of the inner cylinder). Then with

$$Re \equiv \omega_1 R_1^2/\nu, \tag{1.2a}$$

$$\delta \equiv \Delta/R_1, \tag{1.2b}$$

$$\eta \equiv R_1/R_2, \tag{1.2c}$$

the Navier–Stokes equations for this flow become

$$u_r + \frac{1}{r} u + w_z = 0, \tag{1.3a}$$

$$\nabla^2 u - \frac{1}{r^2} u - p_r = Re \left[u u_r + w u_z - \frac{1}{r} v^2 \right], \tag{1.3b}$$

$$\nabla^2 v - \frac{1}{r^2} v = Re \left[u v_r + w v_z + \frac{1}{r} u v \right], \tag{1.3c}$$

$$\nabla^2 w - p_z = Re[u w_r + w w_z]. \tag{1.3d}$$

Here ∇^2 is the axisymmetric cylindrical Laplacian

$$\nabla^2 \equiv \frac{\partial^2}{\partial r^2} + \frac{1}{r}\frac{\partial}{\partial r} + \frac{\partial^2}{\partial z^2}.$$

The inner cylinder is to rotate and the outer cylinder will be at rest. Thus the boundary conditions on the cylinders are:

$$u(1, z) = 0, \qquad v(1, z) = 1, \qquad w(1, z) = 0; \tag{1.4a}$$

$$u(1+\delta, z) = 0, \qquad v(1+\delta, z) = 0, \qquad w(1+\delta, z) = 0. \tag{1.4b}$$

Periodicity in the z-direction is imposed by requiring

$$u\left(r, \frac{\pi}{k}\right) = u\left(r, -\frac{\pi}{k}\right), \qquad v\left(r, \frac{\pi}{k}\right) = v\left(r, -\frac{\pi}{k}\right),$$
$$w\left(r, \frac{\pi}{k}\right) = w\left(r, -\frac{\pi}{k}\right), \qquad p\left(r, \frac{\pi}{k}\right) = p\left(r, -\frac{\pi}{k}\right). \tag{1.4c}$$

2. Numerical Methods

2A. *Fourier Decomposition*

To approximate the solutions of (1.3), (1.4) we first expand in finite Fourier series in the z-direction. The coefficients in these expansions depend on r and finite differences are used to approximate them. Specifically we seek solutions in the form

$$p(r, z) = \sum_{j=0}^{N} p_j(r) \cos jkz, \qquad u(r, z) = \sum_{j=0}^{N} u_j(r) \cos jkz,$$
$$v(r, z) = \sum_{j=0}^{N} v_j(r) \cos jkz, \qquad w(r, z) = \sum_{j=1}^{N} w_j(r) \sin jkz. \tag{2.1}$$

Thus p, u, v are assumed even in z while w is odd. This last assumption and the periodicity in (1.4c) implies that $w(r, \pm\pi/k) = 0$ so no fluid flows across the planes $z = \pm\pi/k$.

We insert expansions (2.1) into (1.3) and use the orthogonality of the trigonometric functions on $[-\pi, \pi]$ (i.e., Galerkin's method) to get, for $j = 0, 1,..., N$ in (2.2a)–(2.2c) and for $j = 1, 2,..., N$ in (2.2d),

$$u_j' + \frac{1}{r} u_j + jkw_j = 0, \tag{2.2a}$$

$$-u_j'' - \frac{1}{r} u_j' + \left[(jk)^2 + \frac{1}{r^2}\right] u_j + p_j' = Re\, f_{1j}(\mathbf{U}, \mathbf{U}', \mathbf{V}, \mathbf{W}; r), \tag{2.2b}$$

$$-v_j'' - \frac{1}{r} v_j' + \left[(jk)^2 + \frac{1}{r^2}\right] v_j = Re\, f_{2j}(\mathbf{U}, \mathbf{V}, \mathbf{V}', \mathbf{W}; r), \tag{2.2c}$$

$$-w_j'' - \frac{1}{r} w_j' + (jk)^2 w_j - jkp_j = Re\, f_{3j}(\mathbf{U}, \mathbf{W}, \mathbf{W}'; r). \tag{2.2d}$$

Here primes denote r-differentiation. The coefficients, grouped as the vector $\mathbf{U} \equiv (u_0, u_1, ..., u_N)$, etc., enter into the functions f_{ij} quadratically; for example,

$$f_{1j}(\mathbf{U}, \mathbf{U}', \mathbf{V}, \mathbf{W}; r)$$
$$\equiv \int_{-\pi/k}^{\pi/k} \cos jkz \left[uu_r + wu_z - \frac{1}{r^2} v^2\right] dz \qquad (1 \leqslant j \leqslant N)$$
$$= \frac{2}{r} v_0 v_j - \frac{1}{2} \left\{ \sum_{n=1}^{j-1} \left[u_n u_{j-n}' + (j-n)\, kw_n u_{j-n} - \frac{1}{r} v_n v_{n-j}\right] \right.$$
$$\left. + \sum_{n=j+1}^{N} \left[u_n u_{n-j}' + u_n' u_{n-j} - (n-j)\, kw_n u_{n-j} - nku_n w_{n-j} - \frac{2}{r} v_n v_{n-j}\right] \right\}. \tag{2.3}$$

The other functions, f_{2j} and f_{3j}, are determined similarly and are given in [12, Eqs. (2.13), (2.14)].

The periodicity boundary conditions (1.4c) are automatically satisfied by expansions (2.1). On $r = 1$ and $r = 1 + \delta$ we get from (2.1) in (1.4a), (1.4b) the boundary conditions

$$u_j(1) = v_j(1) = 0, \quad 1 \leqslant j \leqslant N; \qquad u_0(1) = 0, \qquad v_0(1) = 1; \tag{2.4a}$$

$$\begin{aligned} u_j(1 + \delta) = v_j(1 + \delta) = w_j(1 + \delta) = 0, \qquad 1 \leqslant j \leqslant N; \\ u_0(1 + \delta) = v_0(1 + \delta) = 0. \end{aligned} \tag{2.4b}$$

From (2.2a) with $j = 0$ and $u_0(1) = 0$ it follows that $u_0(r) \equiv 0$. We used this result to eliminate $u_0(r)$ and thus to simplify the program slightly. We also note that only $p_0'(r)$ enters into the Eqs. (2.2) and so $p_0(r)$ is undetermined to within a constant. Thus we arbitrarily set

$$p_0(1) = 0. \tag{2.4c}$$

2B. *Difference Approximations*

System (2.2)–(2.4) is a two-point boundary-value problem but it is not immediately clear that the problem is well posed. To show how well posedness can be established let the $N + 1$ functions $p_j(r)$, $0 \leqslant j \leqslant N$, be given. Then (2.2b)–(2.2d) form a system of $3N + 2$ nonlinear second-order equations for as many unknowns $[u_j(r), v_j(r), w_j(r)]_0^N$ (recalling $w_0(r)$ never enters). In (2.4a), (2.4b) we have $6N + 4$ boundary conditions. So this system is formally consistent (i.e., has the proper number of boundary conditions for a unique solution). The $N + 1$ equations in (2.2a) can then be viewed as constraints which determine the $N + 1$ coefficients $p_j(r)$. In our method the pressure coefficients will be determined simultaneously with the velocity coefficients (by employing Newton's method on the entire system).

We approximate system (2.2)–(2.4) by means of finite differences. Specifically a uniform net $r_m = 1 + mh$, $0 \leqslant m \leqslant M + 1$, with $h = \delta/(M + 1)$ is placed on $[1, 1 + \delta]$. Then in (2.2) we use *centered finite differences* at each r_m, $1 \leqslant m \leqslant M$, so that the scheme has $O(h^2)$ accuracy. Since $u_0(r) \equiv 0$ has been eliminated this yields $2M(2N + 1)$ equations. There are $(6N + 3)$ boundary conditions remaining in (2.4) so we have $(4MN + 2M + 6N + 3)$ equations. However, there are $(4N + 2)(M + 2)$ unknowns and thus $(2N + 1)$ additional equations are required for a determined system. To get them we eliminate u_j'' from (2.2b) by adding to it the r-derivative of (2.2a). The resulting $N + 1$ equations are

$$p_j' + (jk)^2 u_j + (jk) w_j' = Re\, f_{1j}(\mathbf{U}, \mathbf{U}', \mathbf{V}, \mathbf{W}; r), \qquad 0 \leqslant j \leqslant N. \tag{2.5}$$

These are first order and we difference them at $r_0 + h/2$ and $r_M + h/2$ using the midpoint rule. This gives $2N + 2$ additional equations but we drop the equation for $j = 0$ at $r_0 + h/2$. These difference relations are sometimes referred to as the "pressure boundary conditions," but there is no real justification for that terminology. There are many other ways in which the missing $2N + 1$ constraints could have been imposed. But some numerical experiments done on Couette flow indicate that the above procedure is best.

The difference equations form a nonlinear algebraic system of $(2N + 1)(2M + 1)$ equations and unknowns when the specified values of the $(6N + 3)$ quantities in the boundary conditions (2.4) are eliminated [we do not count $u_0(r_0)$ and $u_0(r_{M+1})$ here as they have been eliminated previously]. These equations can be written in the vector form

$$\mathbf{G}(\mathbf{x}, Re) = A\mathbf{x} - Re\,\mathbf{F}(\mathbf{x}) - \mathbf{b} = 0. \tag{2.6}$$

Here A is a block tridiagonal matrix, $\mathbf{x}$ is some ordering of the unknowns on the net, $\mathbf{F}(\mathbf{x})$ represents the difference forms of the f_{ij} on the net, and $\mathbf{b}$ is the forcing term due to the boundary condition $v_0(1) = 1$. A more detailed discussion of the ordering and structure of A is given in [12]. It has a block tridiagonal structure and in the computations it is treated as a band matrix of bandwidth $(10N + 5)$.

2C. *Solution Procedures*

The discrete system (2.6) is solved using the pseudoarclength continuation method of [7, 8]. In particular, these techniques are efficient for continuing in the Reynolds number, Re, and for determining bifurcating branches of solutions. The basic idea is to consider a curve or branch of solutions, $[\mathbf{x}(s), Re(s)]$, parametrized by some new parameter, s (essentially arclength). Then if the solution is known at $s = s_0$, say, and we have determined the "tangent" $[\dot{\mathbf{x}}(s_0), \dot{Re}(s_0)]$ to the solution curve, a predicted value of the solution at $s = s_0 + \Delta s$ is

$$[\mathbf{x}^0(x), Re^0(s)] = [\mathbf{x}(s_0), Re(s_0)] + \Delta s[\dot{\mathbf{x}}(s_0), \dot{Re}(s_0)]. \tag{2.7}$$

This is used as the initial guess in Newton's method to solve (2.6) and the adjoined pseudoarclength condition

$$\langle(\mathbf{x}(s) - \mathbf{x}(s_0)), \dot{\mathbf{x}}(s_0)\rangle + (Re(s) - Re(s_0)) \cdot \dot{Re}(s_0) = \Delta s. \tag{2.8}$$

After the new solution is obtained the new tangent vector is easily computed and the procedure is continued.

The possible occurrence of bifurcation is signaled by the change in sign of the determinant of the Jacobian matrix

$$\frac{\partial \mathbf{G}}{\partial \mathbf{x}} = A - Re\,\mathbf{F}'(\mathbf{x}). \tag{2.9}$$

When this occurs we first locate accurately the solution $[\mathbf{x}(s), Re(s)]$ at which (2.9) is singular. Then appropriate tests are made to see if bifurcation may occur. If it does we compute the tangent vector to the bifurcating branch of solutions and then continue along this new branch. All the required procedures are described in [7, 12]. The main computational problem in these procedures is the *LU*-factorization of the Jacobian (2.9). This is done using a band structure with bandwidth $(10N + 5)$.

"Newton's method" as we employ it is actually a combination of an occasional true Newton step (i.e., determining a new Jacobian matrix and finding its *LU*-factored form) and several chord or special Newton steps. The latter use the latest previously factored Jacobians. Although much faster, this technique uses more storage so its effectiveness is of course dependent on machine size and problem size. Using $N = 8$ modes with $M = 15$ internal grid points our Jacobian was of order 527 with bandwidth 101. It required about 35 sec to evaluate the matrix elements, about 30 sec. to do the *LU*-decompositions, and about 1 sec for a back substitution. In one case ($Re = 130$, $\eta = 0.5$) a solution was obtained in about 6 to 8 Newton iterations taking about 9 min. When the chord method was introduced a solution was obtained in about 2.7 min. All of these computations were done on the IBM 370/158 at Caltech.

After a solution $[\mathbf{x}(s), Re(s)]$ has been determined the velocity and pressure fields are computed on an appropriate (r, z)-grid. This employs fast Fourier transforms (FFTs) to evaluate the trigonometric sums in (2.1). We thank Prof. B. Fornberg for advice and for providing subroutines for FFTs, field plots, and band elimination.

3. Results of Calculations

Extensive computations have been done on two configurations for which experimental results [4] are available. The outer cylinder is always at rest, $\omega_2 = 0$; the outer radius is fixed at $R_2 = 2$ cm; and two values of the inner radius are used: $R_1 = 1$ cm, $\Delta = 1$ cm (the *wide gap* case), and $R_1 = 1.9$ cm, $\Delta = 0.1$ cm (the *narrow gap* case). Different fluids were used in each case and by varying the inner angular velocity ω_1 a wide range of Reynolds numbers were covered. Some of the results, showing bifurcation from Couette flow, are presented in terms of graphs (Figs. 1 and 3) of Reynolds number based on gap width, Re^δ, versus an average torque. From (1.2) we have that

$$Re^\delta \equiv \frac{\omega_1 R_1 \Delta}{\nu} = Re\ \delta. \tag{3.1}$$

The experimental cylinders were 10 cm long and the torque was measured on the middle 5cm of the outer cylinder, to reduce end effects. To compute the average torque at radius r on a portion of cylinder of length H we use, in a combination of dimensional and dimensionless variables,

$$G(r) = 2\pi r^2 H \rho \nu^2\ Re \left[\frac{v_0(r)}{r} - \frac{dv_0(r)}{dr}\right]. \tag{3.2}$$

Here ν is the kinematic viscosity and ρ is the density of the fluid. For exact steady-state solutions $G(r)$ should be independent of r. We computed $G(r)$ at $r_{1/2} = 1 + h/2$ and at $r_{M+1/2} = 1 + \delta - h/2$ to maintain $O(h^2)$ accuracy. The values $G(r_{1/2})$ are used in the graphs and we generally found that $G(r_{M+1/2}) - G(r_{1/2}) \equiv \Delta G > 0$. As the

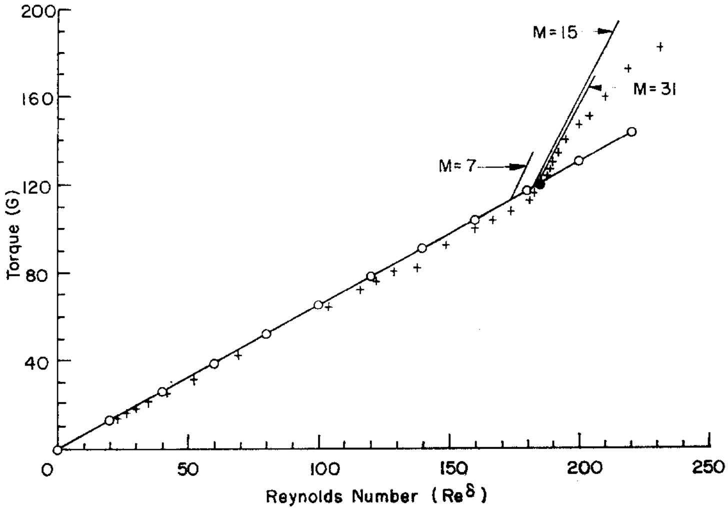

FIG. 1. Torque vs Re^{δ} for narrow gap case: $R_1 = 1.9$, $R_2 = 2.0$, $L/\Delta = 2.007$. Experiments of [4]: +; Couette flow: ○; present calculations: ——; accurate computed bifurcation point: ●, $M = 80$. Three computations of the bifurcating branch are shown, each using a different number M of interior net points.

mesh was refined $|\Delta G|$ decreased. In the narrow gap case we observe $|\Delta G|/G(r_{1/2}) < 0.5\%$ for $M = 31$ points. In the wide gap case $|\Delta G|/G < 3\%$ for $M = 31$ and $|\Delta G|/G < 7\%$ for $M = 15$.

3A. *Narrow Gap Problem*

The fluid used in these experiments had $\nu = 5.796 \times 10^{-3}$ cm^2/sec, $\rho = 1.585$ g/cm^3 and we note that for this configuration $\eta = 0.95$, $\delta = 1/19$. Calculations were done for a series of Re values while the axial wave number k was fixed at the value $k_{cr} = 59.47$. At this value $Re_{cr}(k)$ has a minimum; see [3] where $(k_{cr}\delta)$ is given. It corresponds to the ratio of period to gap width $L_{cr}/\Delta = 2\pi/(k_{cr}\delta) = 2.007$. Some discussion of the stability of flows with k near k_{cr} is contained in [3, 10].

In Fig. 1 we plot the torque on $H = 5$cm of cylinder versus Re^{δ} from the experiments [4]; from Couette flow; and from our present calculations, $G(r_{1/2})$. There are 22 computed points on the bifurcating branch which used $M = 31$ net points. The branch was also computed using $M = 15$ and $M = 7$ points. Cruder net spacing shifts the bifurcating branch but does not change its slope. The bifurcation point was also determined using $M = 80$ grid points to get $Re_{cr} = 184.86$. Computations near bifurcation used only $N = 2$ Fourier modes. As the amplitudes of the higher modes grow, with increasing Re values, additional modes are included along the bifurcating branch. Two criteria are used for adding modes: (i) if the amplitudes of the highest frequency mode cease to be "small", (ii) if the ratio of maxima of corresponding amplitudes of the highest to next highest mode is greater than 10^{-1}. The short branch with $M = 7$ net points used only $N = 2$ modes for each of 16 values of Re^{δ} in $173.8 \leqslant$

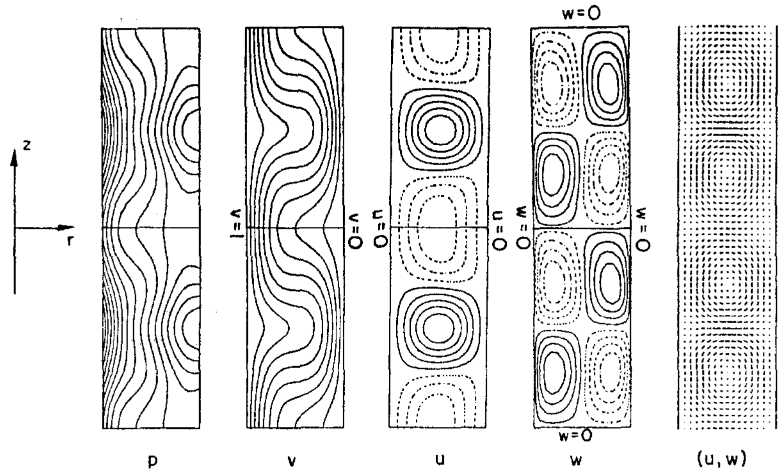

FIG. 2. Level lines of pressure and velocity components in the Taylor vortex flow for the narrow gap case at $Re^{\delta} = 262.28$. These calculations used $N = 6$ modes and $M = 15$ internal net points. The (u, w) vector field in an axial section of the gap is also shown.

$Re^{\delta} \leqslant 182.2$. The longest branch with $M = 15$ net points used $N = 2$ modes for 18 values in $181.94 \leqslant Re^{\delta} < 190.78$, then $N = 4$ modes for 6 values in $189.28 \leqslant Re^{\delta} \leqslant 196.17$, and finally $N = 6$ modes for 12 values in $195.08 \leqslant Re^{\delta} \leqslant 262.28$. (We only show values for $Re^{\delta} \leqslant 214.77$ in Fig. 1, more details are contained in [12, p. 40].) The most accurate branch with $M = 31$ points used $N = 2$ modes for 12 values in $184.21 \leqslant Re^{\delta} \leqslant 188.66$ and $N = 4$ modes for 10 values in $189.28 \leqslant Re^{\delta} \leqslant 205.35$. The deviation between this best computed and the measured curves for $Re^{\delta} > 195$ is most likely due to secondary bifurcation of the actual flow into a nonaxisymmetric state; see [2, 5, 6]. We have not yet included such effects in our calculations. They offer no conceptual difficulties but could not be implemented on the computer used.

Calculations have also been done for a series of k or L/Δ values in $1.46 \leqslant L/\Delta < 2.007$ while holding the Reynolds number Re^{δ} essentially constant (i.e., $203.9 \leqslant Re^{\delta} \leqslant 205.4$). These results show that the radial velocity, $u(r, z)$, has a (negative) minimum at about $L/\Delta = 1.8$. Thus the largest return flow from the outer to the inner cylinder occurs for this case and is in agreement with the experiments of Donnelly and Schwarz for Re^{δ} near 200 reported in [11, p. 1878].

In Fig. 2 we plot level lines of (p, v, u, w) and show the direction field (u, w) for the solution on the bifurcated branch with $L/\Delta = 2.007$ and $Re^{\delta} = 262.28$.

3B. *Wide Gap Problem*

In this case the fluid properites are $\nu = 0.1226$ cm²/sec, $\rho = 0.8404$ g/cm³ and the geometry implies $\eta = 0.5$, $\delta = 1$. More modes and net points are required for an accurate representation of the solutions at higher Re values in this problem. Thus we have only studied the first bifurcating branch and have not examined several two-dimensional equilibria observed in [13].

For the wide gap $Re_{cr}(k)$ has a minimum at $k = k_{cr} = 3.16$ or $L/\Delta = 1.988$; see [3]. With this fixed value we easily compute the Couette flow branch and find a bifurcation at $Re_{cr} = 68.113$. For this accurate determination of Re_{cr} we use $M = 63$ points and $N = 2$ modes. The bifurcating branch was computed using $M = 31$ points and $N = 4$ modes for $Re^\delta \leqslant 73$. With $M = 15$ points we used $N = 4$ modes for $67.25 < Re^\delta \leqslant 81.18$, then $N = 6$ modes for $81.18 < Re^\delta \leqslant 101.76$, and finally $N = 8$ modes up to $Re^\delta = 280.99$. Some of these results are shown in Fig. 3, were the computed torque vs Re^δ is plotted along with the experimentally measured values and the Couette flow values. Computed values are shown up to $Re^\delta = 130$ and nine points are included here. Six further values were computed up to $Re^\delta = 280.99$, where $G(r_{1/2}) = 588.958$ was obtained (see [12, p. 52] for a complete table of values).

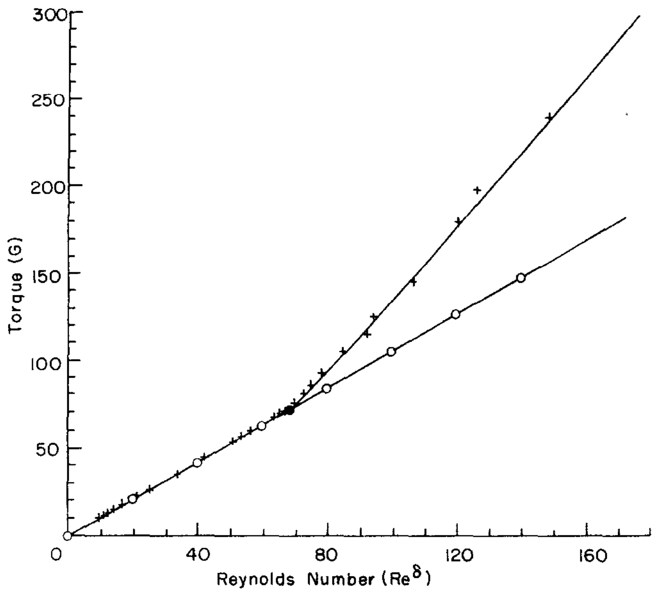

FIG. 3. Torque vs Re^δ for wide gap case: $R_1 = 1.0$, $R_2 = 2.0$, $L/\Delta = 1.988$. Experiments of [4]: +; Couette flow: ○; present calculations: ——; accurate computed bifurcation point: ●, $M = 63$. The bifurcating branch computations used $M = 31$ net points for $Re^\delta \leqslant 73$ and $M = 15$ net points above.

Calculations with fixed $Re^\delta = 101.8$ have been done for eight values of L/Δ in $1.288 \leqslant L/\Delta \leqslant 1.988$. It was found that the torque on 5 cm has a maximum at about $L/\Delta = 1.688$. Such maxima have also been reported at Re^δ values up to 79.4 in [3].

Finally in Fig. 4 we show contour plots of (p, v, u, w) and the vector field (u, w) for the wide gap solution on the bifurcated branch for $L/\Delta = 1.988$ at $Re^\delta = 280.99$. These results are intended to show the qualitative behavior of the flow at the highest Re^δ value for which we computed with at least 15 net points. The high-frequency wiggles are introduced by the plotting procedure. They are indicative of large gradients and thus suggest the need for finer meshes. Also the number of Fourier modes was not

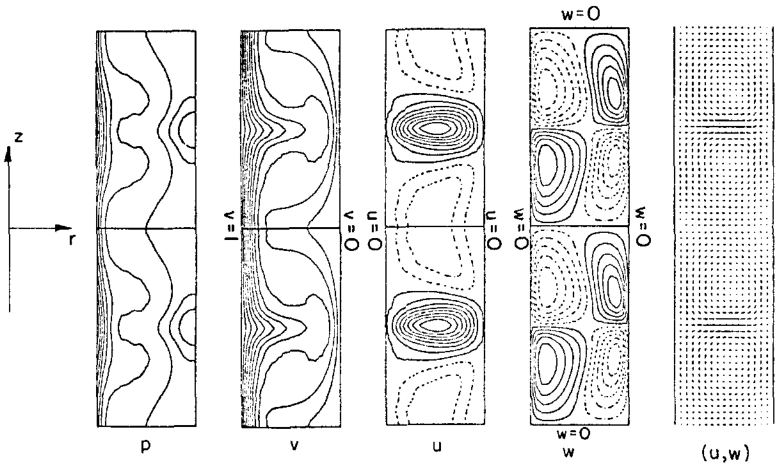

FIG. 4. Level lines of pressure and velocity components in the Taylor vortex flow for the wide gap case at $\mathrm{Re}^{\delta} = 280.99$. These calculations used $N = 8$ modes and $M = 15$ internal net points. The (u, w) vector field in an axial section of the gap is also shown.

sufficient as all computed coefficients were of comparable orders showing that some absent modes were nonnegligible. However, the corresponding plots for $Rz^{\delta} \leqslant 127$ were quite smooth, similar to those of Fig. 2 for the narrow gap case, and we believe the calculations in that range are quite accurate.

REFERENCES

1. D. COLES, *J. Fluid Mech.* **21** (1965), 385–425.
2. A. DAVEY, R. C. DIPRIMA, AND J. R. STUART, *J. Fluid Mech.* **31** (1968), 17–52.
3. R. C. DIPRIMA AND P. M. EAGLES, *Phys. Fluids* **20** (1977), 171–175.
4. R. J. DONNELLY AND N. J. SIMON, *J. Fluid Mech.* **7** (1960), 401–418.
5. P. M. EAGLES, *J. Fluid Mech.* **49** (1971), 529–550.
6. P. M. EAGLES, *J. Fluid Mech.* **62** (1974), 1–9.
7. H. B. KELLER, *in* "Applications of Bifurcation Theory" (P. Rabinowitz, Ed.), pp. 359–384, Academic Press, New York, 1977.
8. H. B. KELLER, *in* "Recent Advances in Numerical Analysis" (C. de Boor and G. H. Golub, Eds.), pp. 73–94, Academic Press, New York, 1978.
9. K. KIRCHGÄSSNER AND P. SORGER, *Quart. J. Mech. Appl. Math.* **22** (1969), 183–209.
10. K. KIRCHGÄSSNER, *in* "Applications of Bifurcation Theory" (P. Rabinowitz, Ed.), pp. 149–174, Academic Press, New York, 1977.
11. K. A. MEYER, *Phys. Fluids* **10** (1967), 1874–1879.
12. R. MEYER-SPASCHE AND H. B. KELLER, "Numerical Study of Taylor-Vortex Flows between Rotating Cylinders," Applied Mathematics Report, California Institute of Technology, Pasadena, 1978.
13. H. A. SNYDER, *J. Fluid Mech.* **35** (1969), 273–298.
14. J. T. STUART, *in* "Applications of Bifurcation Theory" (P. Rabinowitz, Ed.), pp. 127–148, Academic Press, New York, 1977.
15. W. VELTE, *Arch. Ration Mech. Anal.* **22** (1966), 1–14.